Geophys. J. Int. (1994) **117**, 196–204

Interpretation of long-period magnetotelluric soundings in Friuli (north-east Italy) and the electrical characteristic of the lithosphere

C. Braitenberg,[1] P. Capuano,[2] P. Gasparini[2] and M. Zadro[1]

[1] *Istituto di Geodesia e Geofisica, Universita' di Trieste, Via Universita' 7, 34124 Trieste, Italy*

[2] *Dipartimento di Geofisica e Vulcanologia, Universita' Federico II, Largo S. Marcellino 10, 80138 Napoli, Italy*

Accepted 1993 September 2. Received 1993 July 29; in original form 1992 November 13

SUMMARY

One-year-long records of two magnetotelluric (MT) stations, located in the seismic Friuli region (north-east Italy), were analysed in the 60–28 800 s period range. The aim was the investigation of the deep lithospheric electric structure. The computation of the impedances was made by an iterative signal-to-noise enhancing method. Impedances were analysed with complex singular value decomposition (SVD). Some tests were made trying to consider the distortion due to the shallow inhomogeneities. 1-D inversion of the apparent resistivity curves was carried out. The models obtained indicate that the lithosphere thickens from 90 to 120 km westward, in agreement with surface-wave inversion. The westernmost sounding, located in an area of thickened crust, indicates the presence of a ~10 km thick intracrustal conductor, which may be associated with incipient melting of lower crustal rocks.

Key words: electrical resistivity, inversion, Italy, lithosphere, magnetotellurics.

INTRODUCTION

The Istituto di Geodesia e Geofisica of the University of Trieste and the Polish Academy of Sciences carried out a magnetotelluric (MT) campaign in the seismically active Friuli region (north-east Italy) with the hope of detecting anomalous features of the magnetotelluric (MT) and/or of the telluric (T) field which could be correlated with seismic events.

MT and T fields were continuously recorded from July 1987 to June 1988 in two MT stations (Fig. 1). Zadro *et al.* (1988, 1990) published the time variations obtained by analysis of one-component impedance; Braitenberg & Zadro (1990) published the results of 2-D impedance calculations and polarization analysis.

In this paper we use the MT data to compute the resistivity–depth function using 1-D models to invert apparent resistivity and phase curves. The objective of this study was to obtain information on the presence of intracrustal conductive layers and on the thickness of the lithosphere.

Resistivity data relative to the deep continental lithosphere are quite scarce. MT soundings rarely penetrate deeper than the Moho (see, e.g. Stanley, Mooney & Fuis 1990; Klein 1991). Very long-period MT investigations (with periods up to several days or months; see e.g. Egbert & Booker 1992) and geomagnetic C-response studies (e.g. Olsen 1992) have been carried out for investigating the mantle. These data do not have an appropriate resolution at depths lower than 200 km, which are of interest for the electric study of the continental lithosphere and the lithosphere–asthenosphere boundary. Our data therefore fill a gap between crustal and sublithospheric mantle deep ranges.

INSTRUMENTATION

MT stations FDS (Latitude 46°23′N, Longitude 12°40′E) and IAI (Latitude 46°06°N, Longitude 13°33′E) were equipped each with a three-component Torsion–Photoelectric Magnetometer (Jankowski *et al.* 1984) and a T recording system consisting of N–S and E–W trending, 50–100 m long, electric lines, using non-polarizing ceramic Cu–$CuSO_4$ electrodes. The vertical magnetic component will not be used in the following as it was severely affected by interruptions and breakdowns. Data were recorded on magnetic tape with a 20 s sampling interval.

DATA SELECTION

The considered data set ranges from 1987 September to 1988 March. In particular, 4 hr, 24 hr and 144 hr long sequences were selected from the data set for impedance calculation over three different frequency intervals. The analysed time sequences are listed in Table 1.

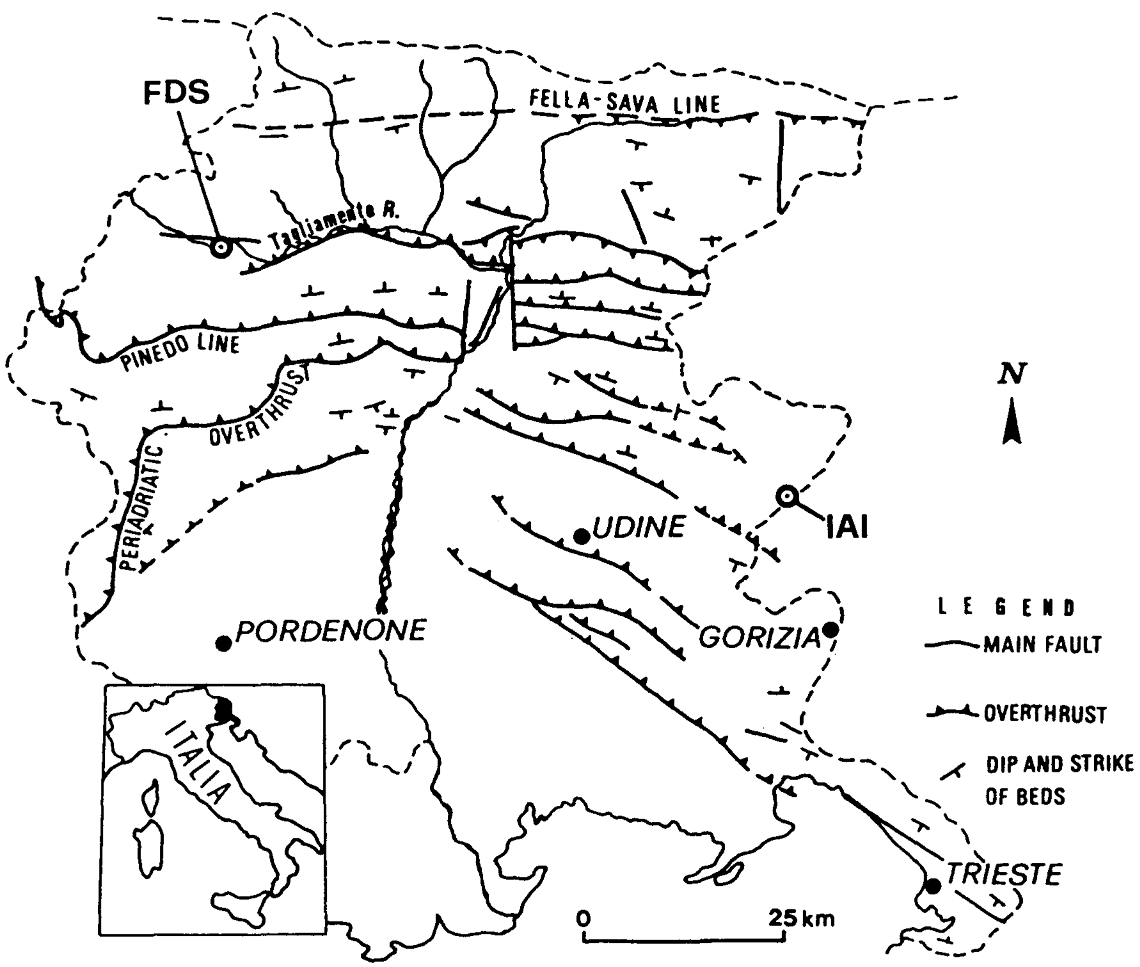

Figure 1. Map of Friuli seismic area (after Slejko *et al.* 1987). The positions of the two MT stations Iainich (IAI) and Forni di sotto (FDS) are indicated.

Table 1. Time sequences selected for the analysis.

The days during which 4 hr or 24 hr long sequences were selected are the following:

1987	September:	8, 11, 12, 13, 14, 15, 16, 17
	December:	14, 15, 16, 17, 18, 19, 24
1988	January:	8, 14, 15, 16, 17, 21, 22
	February:	3, 5, 6, 8, 17, 21, 25
	March:	6, 7, 8, 14, 15

The 144 hr long sequences were selected over the following time intervals:

1987	September:	7–21
1988	January:	8–15, 23–31
	February:	9–25
	March:	10–16

IMPEDANCE AND DERIVED QUANTITIES

If $e(f)$, $b(f)$ are the horizontal components of the T- and B-field respectively, in the frequency domain, the 2-D horizontal 2×2 impedance matrix $Z(f)$ of the structure is defined by:

$$e(f)=Z(f)\cdot b(f).$$

The computation of $Z(f)$ was accomplished by an iterative signal-to-noise enhancing method (Braitenberg & Zadro 1990), which in principle has some analogies with the technique developed by Kao & Rankin (1977). In the nth step the impedance is calculated from the relation:

$$|e_{n-1}(f)-Z_n(f)\cdot b_{n-1}|^2=\min.$$

The predicted T-field is then defined by:

$$e_n(f)=(1-q)\cdot e_{n-1}(f)+qZ_n(f)\cdot b_{n-1}(f),$$

where q is the signal enhancing parameter.

The admittance $Q(f)$ is then obtained from:

$$|b_{n-1}(f)-Q_n(f)\cdot e_n|^2=\min.$$

The predicted B-field is then defined by:

$$b_n(f)=(1-q)\cdot b_{n-1}(f)+qQ_n(f)\cdot b_{n-1}(f).$$

The optimal number of iterations that are to be applied depends on the initial signal-to-noise ratio of the data.

The impedance is analysed with complex Singular-Value Decomposition (SVD), which has been shown to be a general parametrization of Z (Yee & Paulson 1987) and belongs to the class of mathematical decomposition (Groom & Bailey 1991). The SVD (La Torraca, Madden & Korringa

Table 2. Sampling frequencies.

sequence length	sampling	frequency interval	
6 days	900 sec.	$f_1 = 1/27600$ Hz	$f_2 = 1/9780$ Hz
1 day	120 sec.	$f_1 = 1/6600$ Hz	$f_2 = 1/840$ Hz
4 hours	20 sec.	$f_1 = 1/780$ Hz	$f_2 = 1/70$ Hz

1986) resulted in:

$$Z(f) \cdot u_1 = \mu_1 \cdot v_1$$

$$Z(f) \cdot u_2 = \mu_2 \cdot v_2$$

where μ_1, μ_2 are the complex singular values. The vectors u_i, v_i $(i = 1, 2)$ are mutually orthogonal and correspond to the Fourier transformation of two particular elliptically polarized states of the B-field (T-field) at a frequency f with polarization direction $\alpha(\beta)$. The angle α retrieves the strike direction in the case of a 2-D structure, whence an index of 3-D of the structure is given by the skew defined by $\gamma = 90 - |\alpha - \beta|$, which measures the deviation from orthogonality of principal T and B directions (Yee & Paulson 1987; Groom & Bailey 1991). Generalized principal resistivities and phases are defined by:

principal resistivities	principal phases
$\rho_1 = 0.2T\,|\mu_1|^2$	$\phi_1 = \text{argument}\,(\mu_1)$
$r_2 = 0.2T\,|\mu_2|^2$	$\phi_2 = \text{argument}\,(\mu_2)$

where T is the period in seconds, the B-field is measured in nT, the T-field in mV km^{-1} and the resistivity in Ω m.

Impedances were calculated for 18 equispaced frequencies in the range from 3.63×10^{-5} to 1.43×10^{-2} Hz (70–27 600 s). The sampling frequencies chosen for the sequence used for the different frequency intervals are reported in Table 2.

Recordings of the B- and T-field obtained in the two stations during January (8–23), sampled at 900 s intervals, are reported in Fig. 2. Recordings of the two fields in January (14–15), sampled at 60 s intervals, are shown in Fig. 3. The generally good agreement of the B-fields recorded at the two stations is evident. The T-field shows sudden uncorrelated jumps which are of unidentified origin. The daily variation in the T-field is not as evident as in the B-field. The strong variation of the B-field recorded on January 14 corresponds to a magnetic storm. Close observation of the B-field allows distinction of periods of higher and lower B-field activity.

In Figs 4 and 5 the average impedances obtained in both stations are given, and the six parameters obtained from the decomposition of impedance (two principal resistivities and adjoint phase-values, skew and strike direction) are plotted. All angles are measured clockwise. Error bars indicate ±rms error of the parameter obtained by error propagation from the rms error of the weighted means of the components of impedance calculated in each subinterval. The weights are given by the signal-to-noise ratio (SNR) of the T-field for each subinterval defined by:

$$\text{SNR} = \frac{|Z(f) \cdot b(f)|^2}{|e(f) - Z(f) \cdot b(f)|^2}.$$

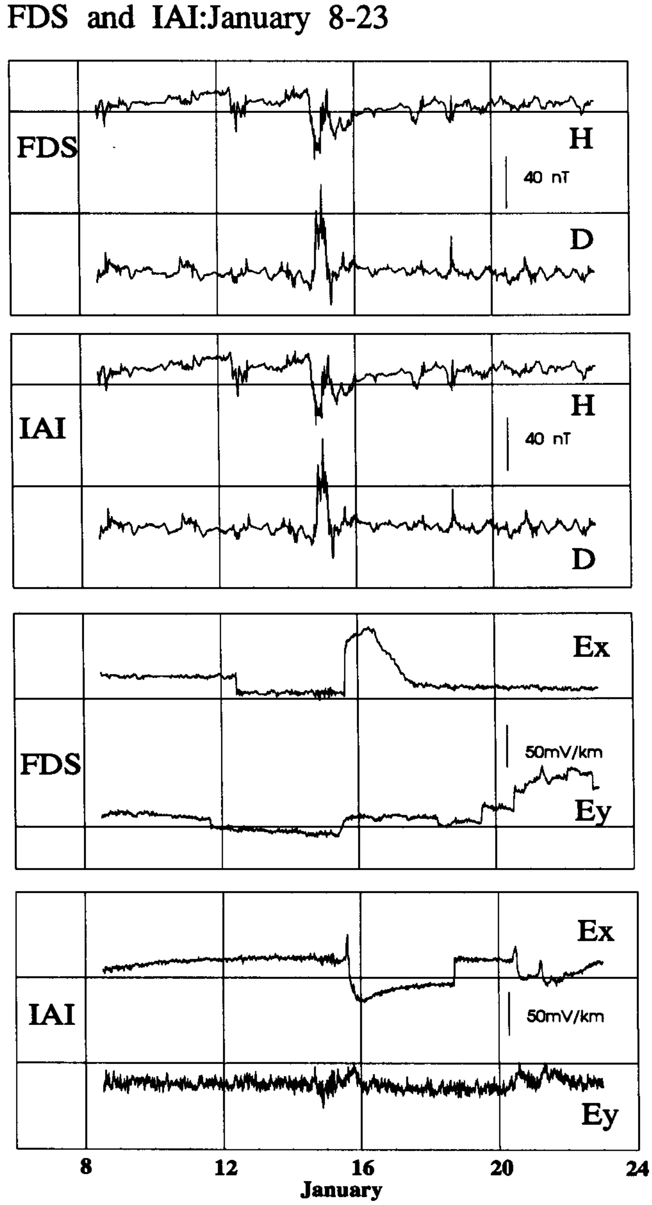

Figure 2. Stations FDS and IAI: recording of B- and T-fields during the month of January (8–23). N–S and E–W components respectively: B-field: H, N–S component; D, E–W component, T-field: E_x N–S component; E_y E–W component. Data decimated to 900 s sampling.

The selection of the subintervals used for the analysis is done according to the criterion of having both high B-field activity (in order to minimize the effect of correlated noise) and high SNR, which indicates a low percentage of uncorrelated noise.

DESCRIPTION OF MT CURVES

Observation of the curves resulting in SVD reveals that the observed impedance does not perfectly satisfy the conditions of 2-D structure (2-D resistivity–phase relationship, zero skew values). Considering the complicated tectonic superficial structure, it is to be expected that a distortion of

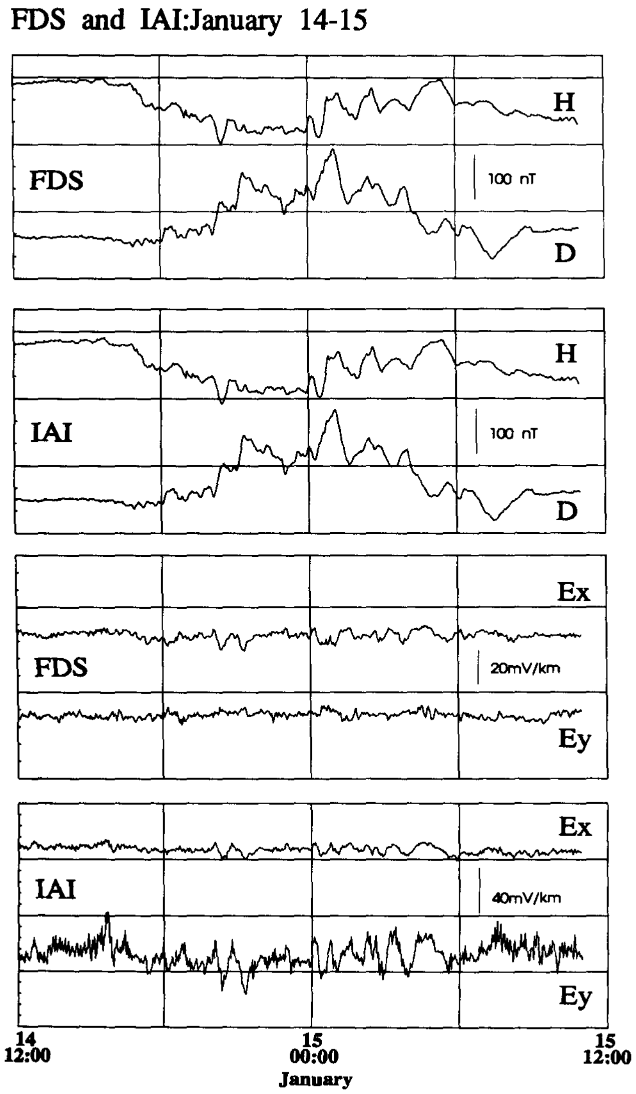

Figure 3. Stations FDS and IAI: recording of B- and T-fields during the month of January (14–15). Field components as in Fig. 2. Data decimated to 60 s sampling.

impedance due to relatively superficial inhomogeneities is present. Retrieval of the regional impedance from the observed tensor is possible, assuming an underlying model regarding the near-surface local inhomogeneities (Bahr 1988; Groom & Bailey 1989). A preliminary analysis considering the distortion present in our data, using the software kindly put at our disposal by Dr K. Bahr, showed that correction for distortion does not considerably alter the final result, through arbitrarily posing restrictive assumptions on the underlying structure. In our case the limited number of stations (two) eliminates the possibility of controlling the correctness of the assumed distortion due to local effects, wherefore we rely on the curves calculated using SVD for the further consideration.

The MT apparent resistivity and phase curves of FDS and IAI stations have quite different patterns. Both soundings show a static shift effect in the two resistivity curves of about one decade.

The FDS apparent resistivity curve has a marked low centred at about 420–600 s and then it increases slowly to an asymptotic value.

The IAI apparent resistivity curve starts from higher values (about 100 Ω m) and decreases to a minimum centred at about 10 000 s.

The IAI sounding has a greater penetration than the FDS sounding due to the higher resistivity of the shallow formations.

MODELLING

Apparent resistivity and phase curves were modelled using a 1-D layered model, imposing that the number of layers needed for fitting the curves should be as small as possible (Fig. 6). The estimate of the model parameter was based on the damped least-squares criterion (Marquardt 1963).

The model gives the average characteristic of the resistivity with depth and should be verified by further MT campaigns involving a much greater number of stations, in order to make 2-D or 3-D modelling possible. In the case of IAI station we used the ρ_2 curve for modelling. In fact, following Bahr & Filloux (1989), an estimate of the correct principal impedances at frequencies corresponding to the first harmonics of the Sq variation, is obtained using the results of the C-response of vertical and horizontal geomagnetic variation. The C-response nearest to our station is the one relative to the station of Fuerstenfeldbruck given for the sixth harmonic of Sq equal to $C = 280 - i164$ km (Olsen 1992), which corresponds to an apparent resistivity $\rho_C = 38\,\Omega$ m and phase $\phi_C = 58°$; comparison with the resistivity observed at IAI shows that the ρ_1 curve is upwards shifted due to local effects, while the value belonging to the ρ_2 curve is in good agreement with this value. In station FDS the impedance was unstable at these lowest frequencies, wherefore calibration of the curve was not possible without further EM measurements. In this case we used the apparent resistivity and phase calculated from the impedance invariant (determinant of the tensor), which has been shown to provide valid results even in regions of three-dimensionality (Ingham 1988; Livelybrooks *et al.* 1989).

The IAI sounding is fitted by a four-layer model, with an essentially resistive layer, ~90 km thick, which is interrupted by a very thin shallow conductor. A deeper conductor is met at about 90 km.

The FDS sounding shows the existence of a thick conductor at a depth of about 10 km. The estimated thickness is about 10 km. Because of the lower upper crustal resistivity this sounding does not penetrate as deep as the IAI sounding. Nevertheless the longest period part of the curve requires the presence of a conductor at a depth of about 120 km for a reasonable fitting.

In Fig. 7 the depth section of a profile in the Eastern Alps (Italian Explosion Seismology Group and Institute of Geophysics, ETH, Zurich, 1981) passing near the two MT stations is shown. The position of the two MT stations has been added to the figure. The features of greatest interest are:

(a) station FDS: presence of a *P*-wave velocity inversion at 10–20 km, overlying an intermediate high-velocity transition layer. The crust/mantle boundary is observed to be at ~45 km depth.

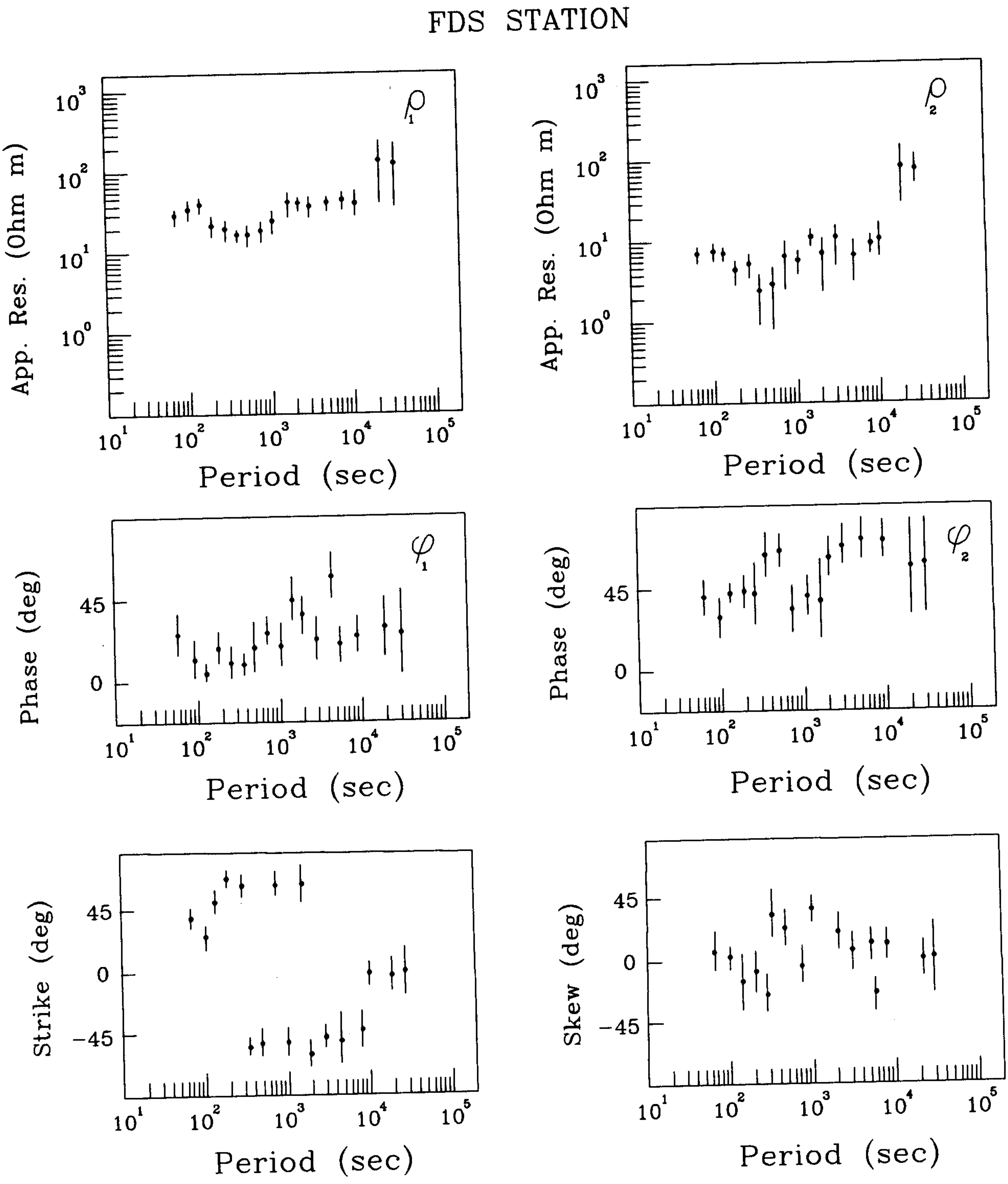

Figure 4. Station FDS: apparent resistivities and phases (ρ_1, ϕ_1, ρ_2, ϕ_2), skew and strike direction for the time interval from 1987 September to 1988 March.

(b) Station IAI: the crust/mantle boundary is at ~30 km depth.

CONCLUSION

The analysis of the nine-months long recording of the MT campaign consisting of two MT stations allowed reliable electric impedance determinations to be obtained, in a region where MT studies have never been accomplished. The data have been analysed in the frequency range 3.63×10^{-5}–1.43×10^{-2} Hz, the highest value being limited by the used sampling frequency (0.05 Hz). In this frequency range the patterns of the curve are determined by the deep resistivity structures.

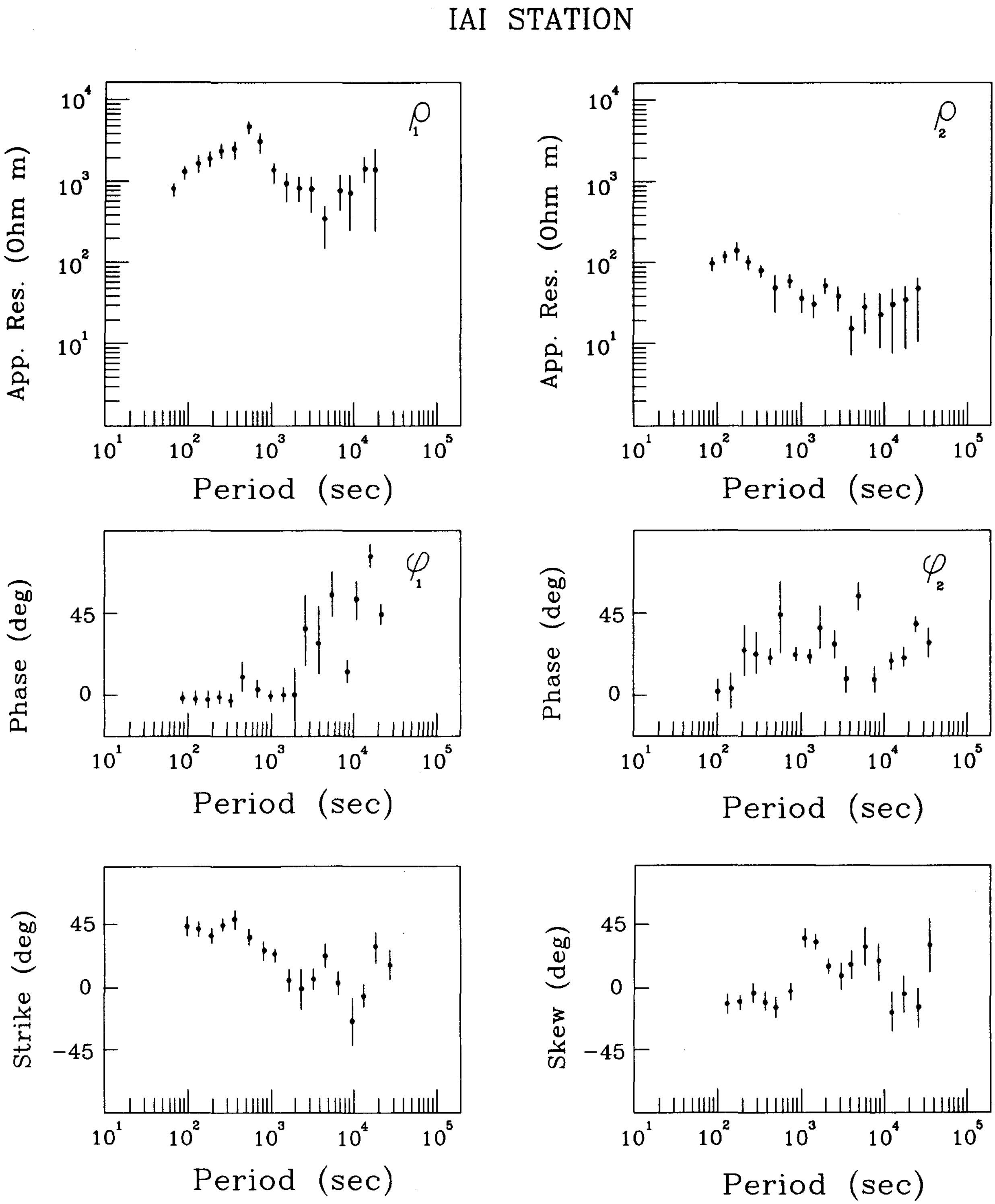

Figure 5. Station IAI: apparent resistivities and phases (ρ_1, ϕ_1, ρ_2, ϕ_2), skew and strike direction for the time interval from 1987 September to 1988 March.

Principal impedance and principal directions were obtained from complex SVD of the calculated impedance matrix, a method convenient to use in a tectonically complicated region, such as Friuli. Due to the presence of noise, an iterative signal-to-noise enhancing method is used for calculating impedance. The duration of the campaign allowed selection of the data for the apparent resistivity determination preponderantly during periods of high magnetic activity, thus minimizing artificial noise.

IAI sounding shows clearly the occurrence of a very thick conductive layer at a depth of ~90 km. The seismic lithosphere thickness in this area, evaluated from surface-

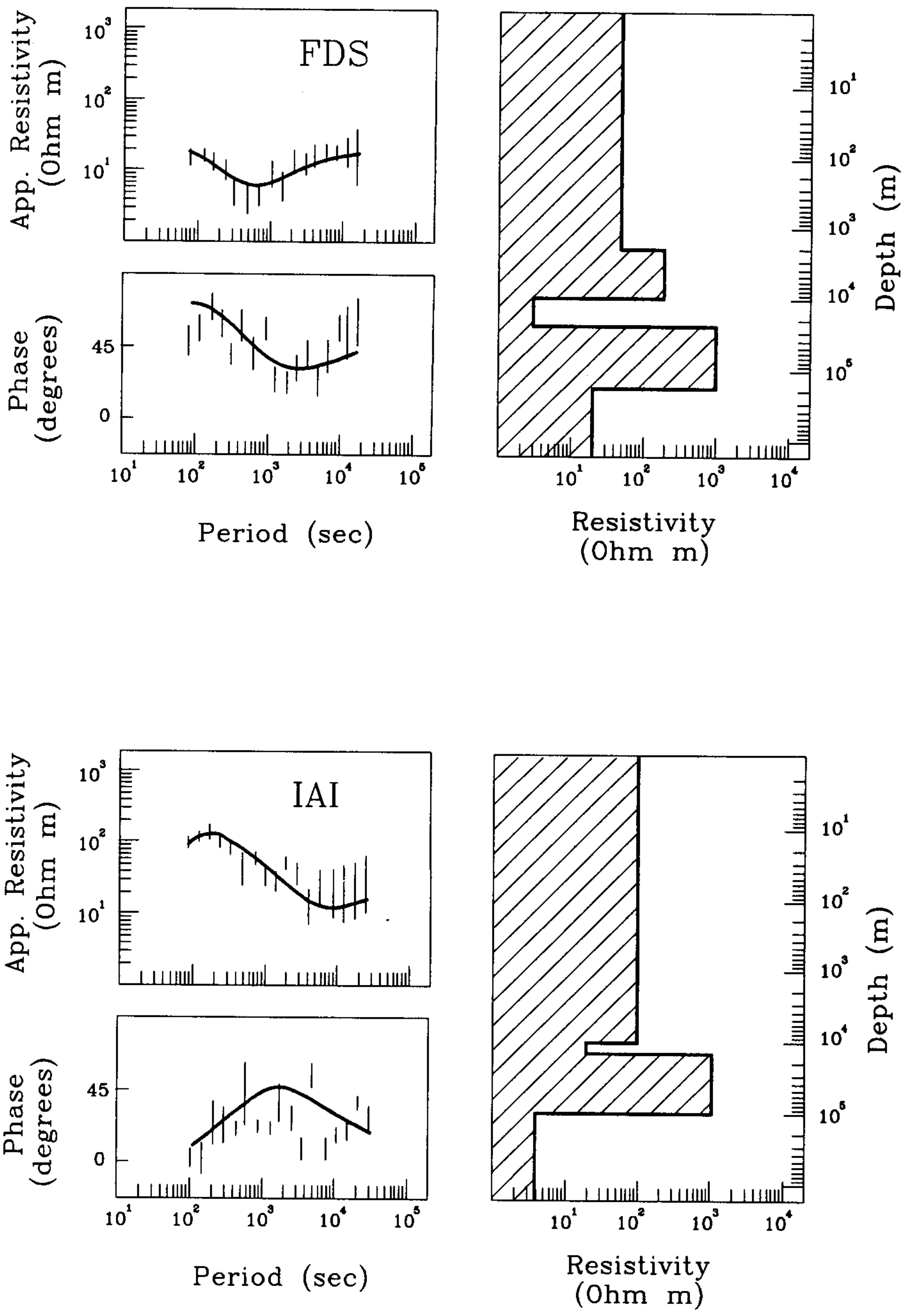

Figure 6. MT 1-D inversion models for IAI and FDS stations. Bold lines on the curve show the apparent resistivities and phases calculated by the proposed models.

wave dispersion, is about the same (Suhadolc, Panza & Mueller 1990). The conductive layer can hence be identified as the upper part of the asthenosphere. The lithosphere appears as a resistive layer having an average resistivity of the order of 100 Ω m down to 10 km of depth, and of 1000 Ω m from ~10 to ~90 km. A few kilometres thick conductive layer may exist at a depth of 10 km. No resistivity variation characterizes the Moho which is at a depth of about 30 km (Italian Explosion Seismology Group 1981).

FDS sounding, on the contrary, shows clearly the occurrence of a thick intracrustal conductive layer between ~10 and 23 km of depth. It coincides with the depth interval where a decrease of *P*-wave velocity was inferred from explosion seismology data (Italian Explosion Seismology Group 1981). The presence of the deep conductor which has been assumed to be the asthenosphere is not as clear as in the IAI sounding. However, a good fitting with the observational data is obtained only if a conductive layer at a depth of about 120 km is assumed.

These results are in good agreement with the existing seismic and geological evidence about the lithospheric structures. Surface-wave data actually indicate a thickening of the lithosphere in the NW direction, consistent with our results. Explosion seismology and geological data indicate that the FDS station is located in an area of crustal

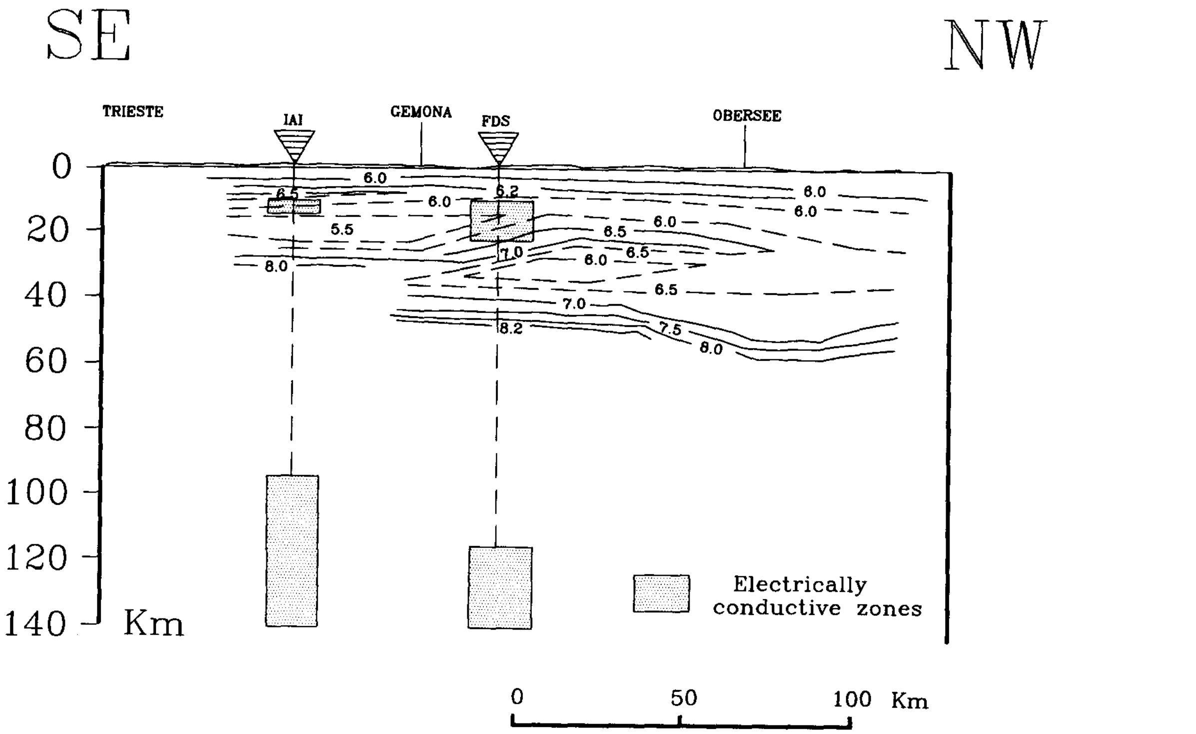

Figure 7. Depth section across the profile Trieste–Obsersee showing the velocity structures from seismic data. The positions of the MT stations are indicated. Electrically conductive zones are shaded.

thickening with respect to the area where the IAI station is located. High electrical conductivities associated with low crustal seismic velocities are generally assumed to be indicative of the occurrence of a small fraction of fluids within the rocks. Silica-rich magmatic fluids, such as those produced by partial melting of crustal rocks, generally have resistivities in excess of 500 Ω m when the water content is lower than 1 per cent. Low resistivities can be obtained only when the fluid contains a significant water fraction as in the early stage of melting (Lebedev & Khitarov 1964; Shankland & Ander 1983). Our results therefore suggest that incipient melting of upper crust occurs where the crust thickens, implying also a possible difference of the thermal states of the crust underlying the two MT stations.

ACKNOWLEDGMENT

This research was supported partially by MURST 40% R91 0209878, 40% R90 020560, 60% R88 020437 and 60% R89 020431, and by MURST 40% R91 00384.

REFERENCES

Bahr, K., 1988. Interpretative regional induction and local distortion, *J. Geophys.*, **62,** 119–127.

Bahr, K. & Filloux, J.H., 1989. Local Sq response functions from EMSLAB data, *J. geophys. Res.*, **94,** 14 195–14 200.

Braitenberg, C. & Zadro, M., 1990. The magnetotelluric campaign in eastern alps, NE-Italy: regional and local 2-D responses of the seismic zone, *Boll. Geof. Teor. Appl.*, **XXXII,** 141–156.

Egbert, G.D. & Booker, J.R., 1992. Very long period magnetotellurics at Tucson observatory: implications for mantle conductivity, *J. geophys. Res.*, **97,** 15 099–15 112.

Groom, R.W. & Bailey, R.C., 1989. Decomposition of magnetotelluric impedance tensors in the presence of local three-dimensional galvanic distortion, *J. geophys. Res.*, **93**(B), 1913–1925.

Groom, R.W. & Bailey, R.C., 1991. Analytic investigation of the effect of near-surface three-dimensional galvanic scatters on MT tensor decomposition, *Geophysics*, **56,** 496–518.

Ingham, M.R., 1988. The use of invariant impedance in magnetotelluric interpretation, *Geophys. J. R. astr. Soc.*, **92,** 165–169.

Italian Explosion Seismology Group, Institute of Geophysics, ETH, Zurich, 1981. Crust and upper mantle structures in the southern alps from deep seismic sounding profiles (1977, 1978) and surface dispersion analysis, *Boll. Geof. Teor. Appl.*, **XII,** 297–330.

Jankowski, J., Marianuk, J., Ruta, A., Sucksdorff, C. & Kivinen, M., 1984. Long-term stability of a torque-balance variometer with photoelectric converters in observatory practice, *Geophys. Surv.*, **6,** 367–380.

Kao, D.W. & Rankin, D., 1977. Enhancement of signal to noise ratio in magnetotelluric data, *Geophysics*, **42,** 103–110.

Klein, D.P., 1991. Crustal resistivity structure from magnetotelluric soundings in the Colorado Plateau–Basin and Range provinces, Central and Western Arizona, *J. geophys. Res.*, **96,** 12 313–12 331.

La Torraca, G.A., Madden, T.R. & Korringa, J., 1986. An analysis of the magnetotelluric impedance for three dimensional conductivity structures, *Geophysics*, **51,** 1819–1829.

Lebedev, E.B. & Khitarov, N.I., 1964. Dependence of the beginning of melting of granite and the electrical conductivity of its melt on high water vapor pressure, *Geochem. Int.*, **1,** 193–197.

Livelybrooks, D.W., Clingman, W., Rygh, J.T., Urquhart, S.A. & Waff, H.S., 1989. A magnetotelluric study of the High Cascade Graben in Central Oregon, *J. geophys. Res.*, **94,** 14 173–14 184.

Marquardt, D.W., 1963. An alghoritm for least squares estimation of non-linear parameters, *SIAM J.*, **11,** 431–441.

Olsen, N., 1992. Day to day C-response estimation for Sq from 1 cpd to 6 cpd using the Z:Y method, *J. geomagn. Geoelect.*, **44,** 433–447.

Shankland, T.J. & Ander, M.E., 1983. Electrical conductivity, temperatures and fluids in the lower crust, *J. geophys. Res.*, **88,** 9475–9484.

Slejko, D., Carulli, G.B., Carraro, F., Csataldini, D., Cavallin, A., Doglioni, C., Iliceto, V., Nicoloch, R., Rebez, A., Semenza, E., Zanferrari, A. & Zanolla, C., 1987. Modello sismotettonico dell'Italia Nord-Orientale. C.N.R., Report N.1, G.N.D.T., U.R.1.4., 'Sismotettonica delle Alpi', Trieste.

Stanley, W.D., Mooney, W.D. & Fuis, C.S., 1990. Deep crustal structure of the Cascade Range and surroundings regions from seismic refraction and magnetotelluric data, *J. geophys. Res.*, **95,** 19 419–19 438.

Suhadolc, P., Panza, G.F. & Mueller, S., 1990. Physical properties of the lithosphere–asthenosphere system in Europe, *Tectonophysics,* **176,** 123–135.

Yee, E. & Paulson, K.V., 1987. The canonical decomposition and its relationship to other forms of magnetotelluric impedance tensor analysis, *J. Geophys.*, **61,** 173–189.

Zadro, M., Santero, P., Ernst, T., Jankowski, J., Marianuk, J. & Teisseyre, R., 1988. A preliminary note on the telluric records in the Friuli seismic zone (North–East Italy), in *Proc. Seminar on the Prediction of Earthquakes,* pp. 1–25, Lisbon, Portugal, 1988 November 14–18.

Zadro, M., Ernst, T., Jankowski, J., Rozluski, C.P. & Teisseyre, R., 1990. Magnetotelluric recordings from the Frilui seismic zone, northeast Italy, *Tectonophysics,* **180,** 303–308.